Research Paper

Identification of noncoding RNA expression profiles and regulatory interaction networks following traumatic spinal cord injury by sequence analysis

Wenzhao Wang[1,2], Yanlin Su[1], Shi Tang[3], Hongfei Li[1], Wei Xie[4], Jianan Chen[1], Lin Shen[1], Xinda Pan[1], Bin Ning[1]

[1]Jinan Central Hospital Affiliated to Shandong University, Jinan, China
[2]Department of Orthopaedics, West China Hospital, Sichuan University, Chengdu, China
[3]Department of Radiology, West China Hospital, Sichuan University, Chengdu, Sichuan, China
[4]Department Emergency Medicine, Affiliated Hospital of Taishan Medical University, Taian, China

Correspondence to: Bin Ning; **email:** ningbin@sdu.edu.cn
Keywords: traumatic spinal cord injury, noncoding RNA, competing endogenous RNA, axonal regeneration
Received: March 11, 2019 **Accepted:** April 10, 2019 **Published:** April 18, 2019

ABSTRACT

Aim: To systematically profile and characterize the noncoding RNA (ncRNA) expression pattern in the lesion epicenter of spinal tissues after traumatic spinal cord injury (TSCI) and predicted the structure and potential functions of the regulatory networks associated with these differentially expressed ncRNAs and mRNAs.
Results: A total of 498 circRNAs, 458 lncRNAs, 155 miRNAs and 1203 mRNAs were identified in TSCI mice models to be differentially expressed. The regulatory networks associated with these differentially expressed ncRNAs and mRNAs were constructed.
Materials and methods: We used RNA-Seq, Gene ontology (GO), KEGG pathway analysis and co-expression network analyses to profle the expression and regulation patterns of noncoding RNAs and mRNAs of mice models after TSCI. The findings were validated by quantitative real-time PCR (qRT-PCR) and Luciferase assay.
Conclusion: noncoding RNAs might play important roles via the competing endogenous RNA regulation pattern after TSCI, further findings arising from this study will not only expand the understanding of potential ncRNA biomarkers but also help guide therapeutic strategies for TSCI.

INTRODUCTION

Spinal cord injury (SCI) is a disabling neurological condition with high economic and social costs; SCI is characterized by the loss of neural tissue and consequent deficits in sensory and motor functions [1]. Each year, half a million people damage their spinal cord, and the injury is almost always life-changing [2]. SCI increases the risk of involuntary movements, bladder and gastrointestinal disorders, and depression [1]. SCI can also be caused by iatrogenic procedures, infection, vascular lesions or tumors, but the most common cause is trauma [3]. Traumatic SCI (TSCI) causes cell necrosis, the disconnection of surviving neurons, and the irreversible interruption of ascending and descending neurotransmission [4]. Unfortunately, recent studies have demonstrated that no effective treatments exist for achieving complete neurological or functional recovery after TSCI. Moreover, the key mechanisms governing the cellular response to injury are largely unknown [5]. A better understanding of the cellular and molecular mechanisms following TSCI is necessary to develop new strategies to promote axonal regeneration and functional recovery.

Noncoding ribose nucleic acids (ncRNAs), which are a class of genetic, epigenetic and translational regulators, have been found to play key roles in various physiological and pathological processes [6]. No less than 70% of the human genome is transcribed, but protein-coding transcripts account for no more than 2%, and extensive transcripts derived from most of the genome generate a large proportion of ncRNAs [7]. Theoretically, ncRNAs do not encode proteins but instead functionally regulate the translation of proteins and can be classified into two types: housekeeping ncRNAs, which consist of small nucleolar RNAs (snoRNAs), small nuclear RNAs (snRNAs), rRNAs, and tRNAs; and regulatory ncRNAs, which consist of microRNAs (miRNAs), long ncRNAs (lncRNAs) with a relatively flexible length of >200 nucleotides, and circular RNAs (circRNAs) with a closed-loop structure [8]. To date, miRNAs are the most extensively studied class of small noncoding RNAs (sncRNAs) [9]; miRNAs are present in a wide range of tissues and fluids [10, 11] and play an essential role in neurological and neurodegenerative diseases by regulating cell-to-cell communication as hormone-like molecules to influence the behaviors of different cells in a paracrine or endocrine manner [12]. Compared to sncRNAs, lncRNAs are more heterogeneous in size, often polyadenylated, longer and lack open reading frames (ORFs). In early studies, the importance of lncRNAs was vastly underestimated because of their low levels of sequence conservation and expression [13]. However, accumulating evidence indicates that lncRNAs play essential roles in the development of diseases in various organisms [14]. In addition, circRNA has recently been identified as a novel type of endogenous ncRNA that is abundant yet enigmatic in mammalian cells. Unlike linear RNAs that are terminated with 5′ caps and 3′ tails, circRNAs are characterized by a covalent closed-loop structure formed by a back-splicing event, without 5′ caps or poly-A tails. Notably, one of the most frequently studied functions of circRNA is the miRNA sponge [15]. Therefore, ncRNAs have potential as candidate diagnostic biomarkers and therapeutic targets in patients with TSCI.

The regulating functions of ncRNAs after TSCI and their underlying functional mechanisms have not yet been sufficiently and systematically described. Therefore, extensive prediction and analysis of the ncRNAs regulating the progression of TSCI is fundamental for the development of understanding the underlying mechanisms and finding effective therapeutic strategies. Our study analyzed the profiles and predicted the function of differentially expressed (DE) ncRNAs in the epicenter of spinal cord lesions in a modified Allen's weight-drop model using RNA sequencing techniques to provide a better comprehending of the diagnostic, prognostic and therapeutic value of ncRNAs.

RESULTS

DE ncRNAs and mRNAs

To identify the effect of TSCI on ncRNA expression in the lesion epicenter, we applied a standard Allen's weight-drop model. SCI mice started to show improvements in locomotor function 2 days after TSCI, but during the first two days, the BMS was rated zero. The BMS of mice in the sham group showed an improvement on day 1 and returned to normal on day 3 postsurgery (Figure 1A). The spinal tissues of inbred C57 mice damaged by Allen's impactor were sliced and stained with H&E. Staining results demonstrated severe damage to the blood-spinal cord barrier and the structural integrity of the lesion epicenter, including rupture, hemorrhage and inflammatory cell infiltration (Figure 1B–1D). To further determine whether ncRNAs were

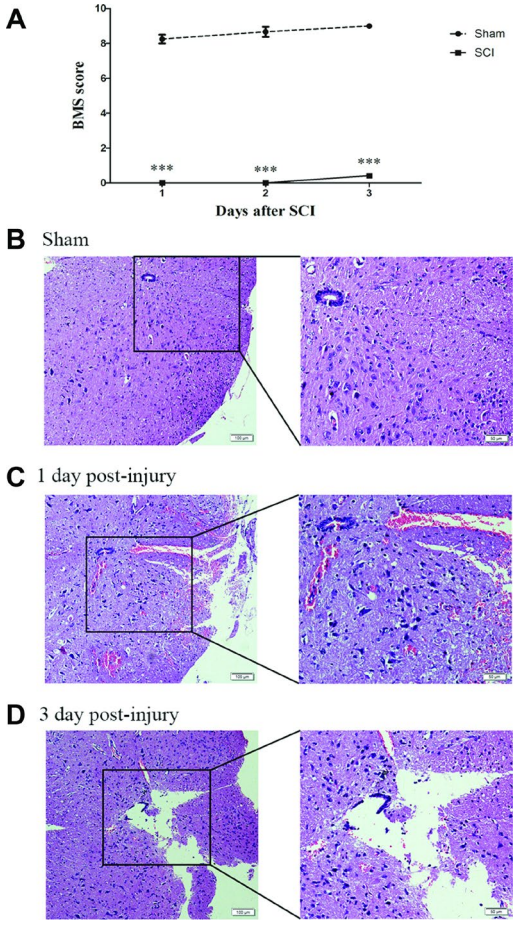

Figure 1. Establishment of SCI animal model. (**A**) BMS scores indicate the motor functional index 3 days after SCI. ***P<0.001. (**B**–**D**) H&E staining of spinal cord samples from the sham and SCI groups at days 1 and 3 postsurgery.

Table 1. Top 40 differently expressed miRNAs in SCI tissues comparing with Sham tissues.

miRNA	Genome ID	Strand	p-value	log2_FoldChange	Regulation
mmu-miR-344e-3p	chr7	−	0.000575	1.33	up
mmu-miR-106b-3p_R-2	chr5	−	0.001598	1.12	up
mmu-miR-5099_L+2R-1	chr12	+	0.002016	2.03	up
mmu-miR-15b-3p	chr3	+	0.002372	0.91	up
mmu-miR-7688-5p	chr10	+	0.003269	2.01	up
mmu-miR-1964-3p	chr7	+	0.004516	1.73	up
mmu-miR-130b-3p	chr16	−	0.004666	1.65	up
mmu-miR-155-5p	chr16	−	0.005421	1.96	up
mmu-miR-27a-5p	chr8	+	0.005929	2.30	up
mmu-miR-18a-3p	chr14	+	0.006440	3.07	up
mmu-miR-18a-5p	chr14	+	0.007264	2.03	up
mmu-miR-223-3p_R+1	chrX	+	0.007287	2.52	up
mmu-miR-214-3p	chr1	+	0.008100	2.37	up
mmu-miR-92a-1-5p	chr14	+	0.009857	3.16	up
mmu-miR-28a-3p	chr16	+	0.010636	0.98	up
mmu-miR-877-5p_R+4	chr17	−	0.011348	0.90	up
mmu-miR-21a-5p_R+1	chr11	−	0.012198	2.46	up
mmu-miR-144-3p_R-1	chr11	+	0.013632	0.87	up
mmu-miR-222-3p_R+2	chrX	−	0.013701	0.91	up
mmu-miR-511-3p	chr2	+	0.013759	1.02	up
mmu-miR-369-3p	chr12	+	0.001349	−0.68	down
mmu-miR-384-3p	chrX	−	0.001676	−0.87	down
mmu-miR-325-5p_R-2	chrX	−	0.002973	−0.49	down
mmu-miR-34a-5p	chr4	+	0.004289	−0.84	down
mmu-miR-383-5p	chr8	−	0.005397	−0.51	down
mmu-miR-128-3p	chr1	+	0.005516	−0.75	down
mmu-miR-30e-5p_R+2	chr4	−	0.006287	−0.67	down
mmu-miR-411-3p_R-1	chr12	+	0.006918	−0.52	down
mmu-miR-329-5p_R+2	chr12	+	0.007447	−0.83	down
mmu-miR-1298-3p	chrX	+	0.009603	−1.07	down
mmu-miR-1264-5p	chrX	+	0.009893	−1.20	down
mmu-miR-135a-5p	chr9	+	0.010159	−0.92	down
mmu-miR-218-5p	chr5	+	0.011109	−0.90	down
mmu-miR-6516-5p_R+3	chr11	+	0.011772	−0.86	down
mmu-miR-488-3p	chr1	+	0.013430	−0.85	down
mmu-miR-7b-5p_R+1	chr17	+	0.013986	−1.00	down
mmu-miR-1843a-3p	chr12	−	0.014024	−0.68	down
mmu-miR-3069-3p	chr12	−	0.015073	−1.37	down
mmu-miR-582-5p	chr13	−	0.015134	−0.90	down
mmu-miR-204-5p	chr19	+	0.015457	−0.77	down

involved in the TSCI, the total RNA of the lesion epicenter at the $T_{8–10}$ level was analyzed by RNA sequencing techniques. P-values <0.05 were used to assess the normalized expression of genes. The dysregulated ncRNAs and mRNAs are shown in a table, cluster map, volcano plot and Venn diagram. Information on the top 40 dysregulated circRNAs, lncRNAs, miRNAs, and mRNAs is listed in order of ascending p-value (Tables 1–4). The cluster map, volcano plot and Venn diagram of DE circRNAs, lncRNAs, miRNAs, and mRNAs after TSCI are shown in Figure 2. According to the data, we summarized the dysregulated RNAs in the TSCI samples compared with those in the sham samples, as follows: 249 circRNAs were upregulated, and 249 circRNAs were downregulated; 356 lncRNAs were upregulated, and 93 lncRNAs were downregulated; 94 miRNAs were upregulated, and 61 miRNAs were downregulated; 1098 mRNAs were upregulated, and 105 mRNAs were downregulated (Figure 3A). DE ncRNAs could directly or indirectly target genes and regulate the expression of target mRNAs. The results of an intersectional analysis of DE circRNAs, lncRNAs, and

Table 2. Top 40 differently expressed CircRNAs in SCI tissues comparing with Sham tissues.

CircRNA ID	Chrom	Gene Name	Strand	p-value	log2_FoldChange	Regulation
circRNA8075	chr14	Diaph3	−	0.000288	3.38	up
circRNA81	chr2	Thbs1	+	0.000459	4.71	up
circRNA172	chr11	Col1a1	−	0.000618	4.71	up
circRNA2355	chr4	Kif2c	−	0.000694	3.73	up
circRNA9086	chr5	Antxr2	−	0.000891	2.02	up
circRNA9357	chr4	Pgd	−	0.000930	2.73	up
circRNA7783	chr15	Racgap1	−	0.001137	2.42	up
circRNA5480	chr13	Nln	−	0.001174	1.10	up
circRNA8879	chr6	Zc3hav1	−	0.001308	2.09	up
circRNA3369	chr2	Atp8b4	−	0.001367	2.88	up
circRNA13618	chr11	Psmd3	+	0.001736	1.06	up
circRNA6169	chr11	Ankfy1	+	0.002037	1.66	up
circRNA8690	chr8	Gm20388	+	0.002183	2.11	up
circRNA8894	chr6	Skap2	−	0.002360	2.31	up
circRNA7312	chr16	Pak2	−	0.002420	1.62	up
circRNA8074	chr14	Diaph3	−	0.002507	3.69	up
circRNA14292	chr5	Gsap	+	0.002621	1.83	up
circRNA7782	chr15	Racgap1	−	0.002623	2.33	up
circRNA8712	chr7	Lig1	+	0.002984	2.66	up
circRNA4569	chr9	Fli1	+	0.003297	1.98	up
circRNA2098	chr4	Anp32b	+	0.003353	1.43	up
circRNA15118	chr1	Dpp10	−	0.000142	−1.36	down
circRNA13219	chr1	Pld5	+	0.002372	−1.41	down
circRNA4130	chr1	Pld5	−	0.000752	−1.51	down
circRNA11130	chr15	Lrrc6	−	0.000863	−2.00	down
circRNA15238	chr18	Nol4	−	0.000946	−1.20	down
circRNA4505	chr9	Cntn5	−	0.001476	−1.46	down
circRNA4277	chr18	Asxl3	+	0.001539	−1.02	down
circRNA1084	chr6	Dync1i1	+	0.001770	−1.13	down
circRNA2986	chr2	Cacna1b	−	0.002072	−1.62	down
circRNA402	chr9	Myrip	+	0.002090	−1.54	down
circRNA7067	chr17	L3mbtl4	+	0.002227	−1.83	down
circRNA2737	chr3	Pogz	+	0.002259	−1.76	down
circRNA4247	chr18	Greb1l	+	0.002611	−1.69	down
circRNA14575	chr4	Rimkla	−	0.002659	−1.64	down
circRNA8251	chr19	Cpeb3	−	0.002934	−1.13	down
circRNA6448	chr11	Tbc1d16	−	0.003047	−1.20	down
circRNA16650	chr14	Sfmbt1	+	0.003097	−1.12	down
circRNA12235	chr12	Dtnb	+	0.003164	−1.10	down
circRNA16513	chr14	Sfmbt1	+	0.003400	−1.14	down

miRNAs and their target DE mRNAs are shown in a Venn diagram (Figure 3B–3D).

Validation of ncRNA and mRNA expression

To validate the reliability of the sequencing data, the changes in the expression of 12 DE ncRNAs and mRNAs, including three circRNAs (circ2464, circ7435, circ7010), three lncRNAs (Gm12840, Gm26809, H19), three miRNAs (miR-21a-5p.R+1, miR-92a-3p.R+1, miR-423-3p) and three mRNAs (Ftl1, Lyz2, Tmsb4x) in the lesion epicenter compared with the sham group were were randomly selected for qRT-PCR analysis (Figure 4B, 4D). All the validated qRT-PCR results of the DE ncRNAs and mRNAs were consistent with the corresponding sequencing data (Figure 4A, 4C).

Enrichment of biological functions and pathway networks

To detect the enrichment categories and to examine the underlying functions of ncRNAs DE after TSCI, DE

Table 3. Top 40 differently expressed lncRNAs in SCI tissues comparing with Sham tissues.

Gene id	Gene name	Status	p-value	log2_FoldChange	Regulation
MSTRG.34122	Homez	novel	0.000005	1.98	up
MSTRG.67284	Tpd52	novel	0.000033	1.30	up
MSTRG.111948	Na	novel	0.000046	2.66	up
MSTRG.74174	Gm15689	novel	0.000054	1.26	up
MSTRG.124087	F630028O10Rik	known	0.000085	1.46	up
MSTRG.40161	Rbfox2	novel	0.000095	1.55	up
MSTRG.113073	Cfap20	novel	0.000109	1.64	up
MSTRG.95251	Gm44170	known	0.000109	1.80	up
MSTRG.93249	Na	novel	0.000159	2.29	up
MSTRG.55738	BE692007	known	0.000189	2.64	up
MSTRG.52721	Dpysl3	novel	0.000225	1.45	up
MSTRG.60157	Arhgap15	novel	0.000269	1.33	up
MSTRG.33815	Na	novel	0.000284	1.62	up
MSTRG.25765	Na	novel	0.000309	2.17	up
MSTRG.77436	Gm11216	known	0.000310	1.53	up
MSTRG.107512	Fgfr2	novel	0.000391	2.08	up
MSTRG.94129	Na	novel	0.000395	1.88	up
MSTRG.11903	Pcbp3	novel	0.000399	1.55	up
MSTRG.123405	Mamld1	novel	0.000421	1.34	up
MSTRG.105294	Na	novel	0.000509	1.61	up
MSTRG.35205	Gm26908	novel	0.000609	1.25	up
MSTRG.14082	Ppm1h	novel	0.000625	1.24	up
MSTRG.33653	NA	novel	0.000954	2.29	up
MSTRG.33653	Thumpd2	novel	0.000987	1.18	up
MSTRG.83712	AI506816	known	0.001001	2.80	up
MSTRG.10902	NA	novel	0.001014	1.60	up
MSTRG.63860	Gm14005	novel	0.001042	1.50	up
MSTRG.110801	Ddx60	novel	0.001081	1.47	up
MSTRG.75978	NA	novel	0.001084	2.21	up
MSTRG.99804	Kcnn4	novel	0.001140	1.92	up
MSTRG.108182	Tacc1	novel	0.001143	1.26	up
MSTRG.28498	Cenpp	novel	0.001203	1.12	up
MSTRG.47244	NA	novel	0.001255	1.63	up
MSTRG.24916	NA	novel	0.001260	2.09	up
MSTRG.125937	Diaph2	novel	0.001263	1.18	up
MSTRG.98701	3300002P13Rik	known	0.000457	−1.34	down
MSTRG.52759	Pcdha6	novel	0.000674	−1.45	down
MSTRG.83528	Pclo	novel	0.000711	−1.02	down
MSTRG.24945	NA	novel	0.000748	−1.47	down
MSTRG.11329	Rhobtb1	novel	0.001009	−1.41	down

NA, not annotated.

ncRNAs and DE mRNAs were subjected to GO and KEGG pathway analyses. DE mRNAs and coexpressed or target mRNAs of DE ncRNAs were identified. The GO molecular function analysis showed that the dysregulated transcripts of ncRNAs were associated with cell division, focal adhesion, proteinaceous extracellular matrix, positive regulation of cell migration, extracellular matrix components, regulation of cell shape, integrin binding, defense response to bacterium and leukocyte cell-cell adhesion (Figure 5A). In addition, the significant GO items indicated that mRNAs DE after TSCI were significantly associated with cytoplasm, protein binding, extracellular exosome, extracellular space, cell surface, focal adhesion, innate immune response and mitotic nuclear division (Figure 5B). Correspondingly, the top 20 ncRNA-associated pathways were demonstrated by KEGG analysis, and the most significantly associated pathways were cytokine-cytokine receptor interaction, cell cycle, leukocyte transendothelial migration, phagosome, Leishmaniasis,

Table 4. Top 40 differently expressed mRNAs in SCI tissues comparing with Sham tissues.

Gene id	Gene name	p-value	log2_FoldChange	Regulation
MSTRG.101002	Snord34	0.000013	1.51	up
MSTRG.80254	Gjb3	0.000025	1.58	up
MSTRG.104414	P2ry6	0.000070	2.41	up
MSTRG.114824	Mmp3	0.000074	2.00	up
MSTRG.65092	H13	0.000074	1.03	up
MSTRG.27838	F13a1	0.000076	2.01	up
MSTRG.13769	Lyz2	0.000086	4.44	up
MSTRG.121761	Ccr1	0.000087	3.38	up
MSTRG.20499	Naglu	0.000129	2.95	up
MSTRG.3656	Ugt1a1	0.000154	1.21	up
MSTRG.107440	F7	0.000177	1.60	up
MSTRG.105998	Nupr1	0.000185	2.18	up
MSTRG.12171	Sbno2	0.000195	1.97	up
MSTRG.111467	Bst2	0.000196	2.64	up
MSTRG.19369	Ccl7	0.000212	3.65	up
MSTRG.28823	Rgs14	0.000221	1.01	up
MSTRG.108769	Msr1	0.000241	4.58	up
MSTRG.117687	Tagln	0.000241	4.68	up
MSTRG.52513	Cd14	0.000243	3.52	up
MSTRG.86784	Cxcl1	0.000244	2.26	up
MSTRG.92027	Flnc	0.000248	1.89	up
MSTRG.6767	Selp	0.000266	1.50	up
MSTRG.31848	Nid2	0.000272	1.27	up
MSTRG.19493	Ccl4	0.000275	1.37	up
MSTRG.104483	Folr2	0.000294	1.84	up
MSTRG.21200	Cd300ld	0.000325	1.72	up
MSTRG.104929	Adm	0.000330	1.32	up
MSTRG.1578	Col5a2	0.000347	1.87	up
MSTRG.100407	Fxyd3	0.000352	2.38	up
MSTRG.33361	Wdfy4	0.000387	1.01	up
MSTRG.89616	Lat2	0.000435	3.08	up
MSTRG.114822	Mmp12	0.000451	1.10	up
MSTRG.34965	Pbk	0.000458	2.92	up
MSTRG.97389	Ptpn6	0.000471	2.19	up
MSTRG.127268	Tmsb4x	0.000488	2.82	up
MSTRG.20948	Milr1	0.000501	2.23	up
MSTRG.40133	Ncf4	0.000508	2.51	up
MSTRG.105902	Il4ra	0.000509	2.79	up
MSTRG.78174	Elavl2	0.000260	-1.28	down

Malaria and Systemic lupus erythematosus pathways, (Figure 5C). In addition, KEGG pathway analysis of DE mRNAs revealed significant associations with cytokine-cytokine receptor interaction, focal adhesion, phagosome, chemokine signaling, Regulation of actin cytoskeleton, lysosome, Cell cycle and Toll-like receptor signaling pathways, among others (Figure 5D).

Regulatory networks of ncRNAs and mRNAs

The network of interactions of the host genes of these DE ncRNAs was also examined to elucidate the molecular mechanisms underlying the pathogenesis of TSCI. Considering that an important biological function of competing endogenous RNAs (ceRNAs) is binding to miRNAs, the binding relationships between ceRNAs and miRNAs were preliminarily determined. The miRNA-binding sites of lncRNAs and circRNAs were identified to construct lncRNA/circRNA–miRNA–mRNA coexpression networks. miRNA was used as the center of each network, which clearly shows possible regulated target genes. The lncRNA/circRNA–miRNA–mRNA interaction networks were conveniently displayed using Cytoscape. Eight DE miRNAs, *i.e.*, miR-23a-5p, miR-

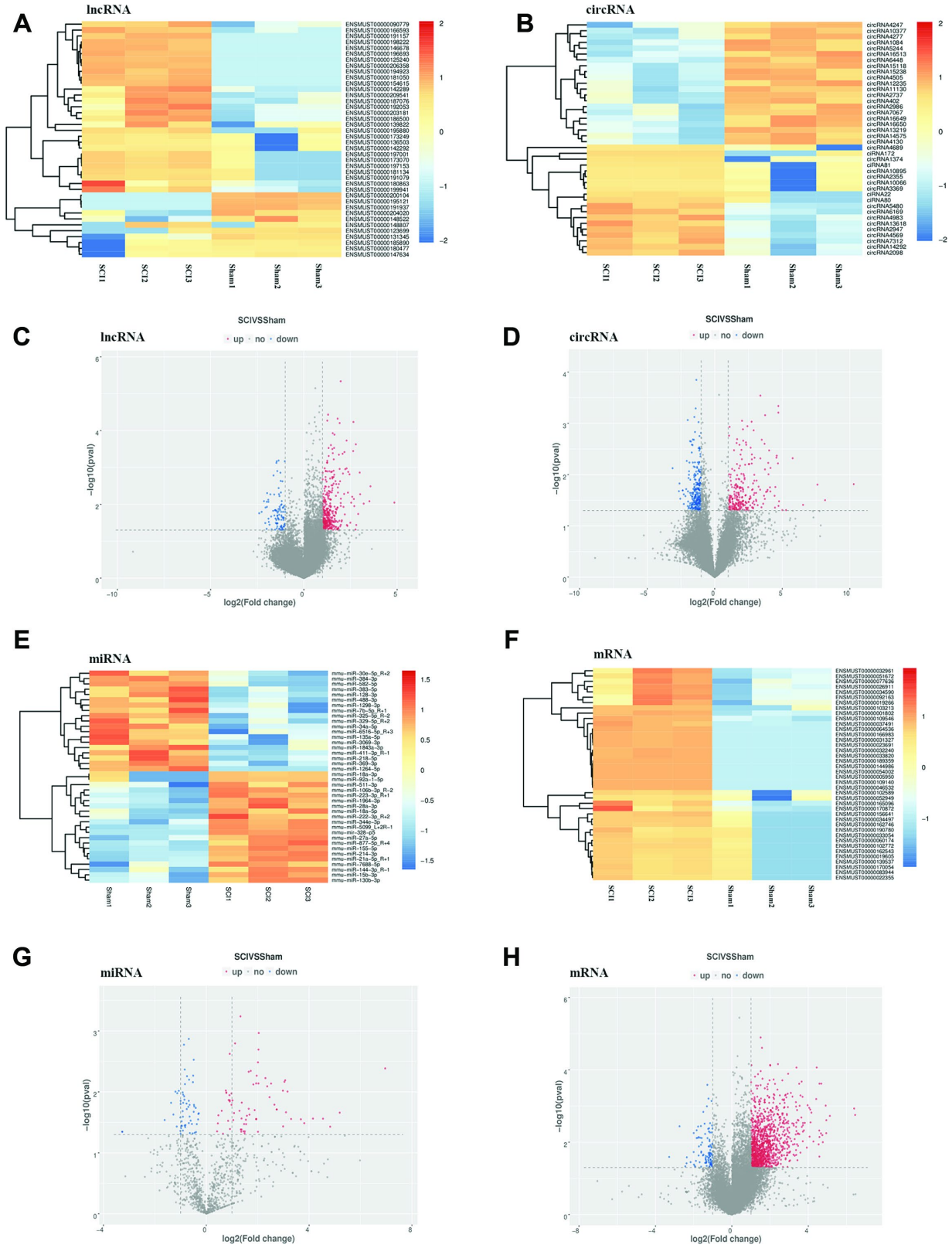

Figure 2. Expression profiles of DE ncRNAs and mRNAs in the lesion epicenter after SCI. (**A**) Heat map of DE lncRNAs in the SCI group compared with the sham group. (**B**) Heat map of DE circRNAs. (**C**) Volcano plot indicating the differential expression of lncRNAs. (**D**) Volcano plot of circRNAs. (**E**) Heat map of DE miRNAs. (**G**) Volcano plot of miRNAs. (**F**) Heat map of DE mRNAs. (**H**) Volcano plot of mRNAs. Up-regulated and down-regulated genes are colored in red and blue, respectively.

222-3p, miR-223-3p, miR-22-5p, miR-218-5p, miR-214-5p, miR-21a-3p, and miR-21a-5p, and their paired ceRNAs and mRNAs were selected as intuitive examples showing parts of the whole complicated network involved in the pathogenesis of TSCI (Figures 6–7). The results show the regulatory relationship between ncRNAs and mRNAs with regard to TSCI. Furthermore, two pairs of binding relationships between ceRNAs and miRNAs were verified with a dual-luciferase reporter system. We found that the overexpression of miR-21-5p significantly decreased the luciferase activity of reporter vectors containing the wild-type lncRNA Gm33755 and circRNA6370 3′-UTR (Figure 8). Collectively, these results establish lncRNA33755 and circRNA6370 as targets of miR-21-5p.

DISCUSSION

With the aging of the world population, increasing numbers of elderly persons are sustaining vertebral compression fractures (VCF) due to osteopenia, 25% of postmenopausal women are affected by a compression fracture during their lifetime, and spinal cord injury is one of the most serious complications of VCF in elderly patients leading to significant morbidity and mortality [16–18].

Since there are no approved therapies for restoring sensation or mobility following TSCI, achieving functional rehabilitation has been among the primary research interests of experimental neuroscientists in

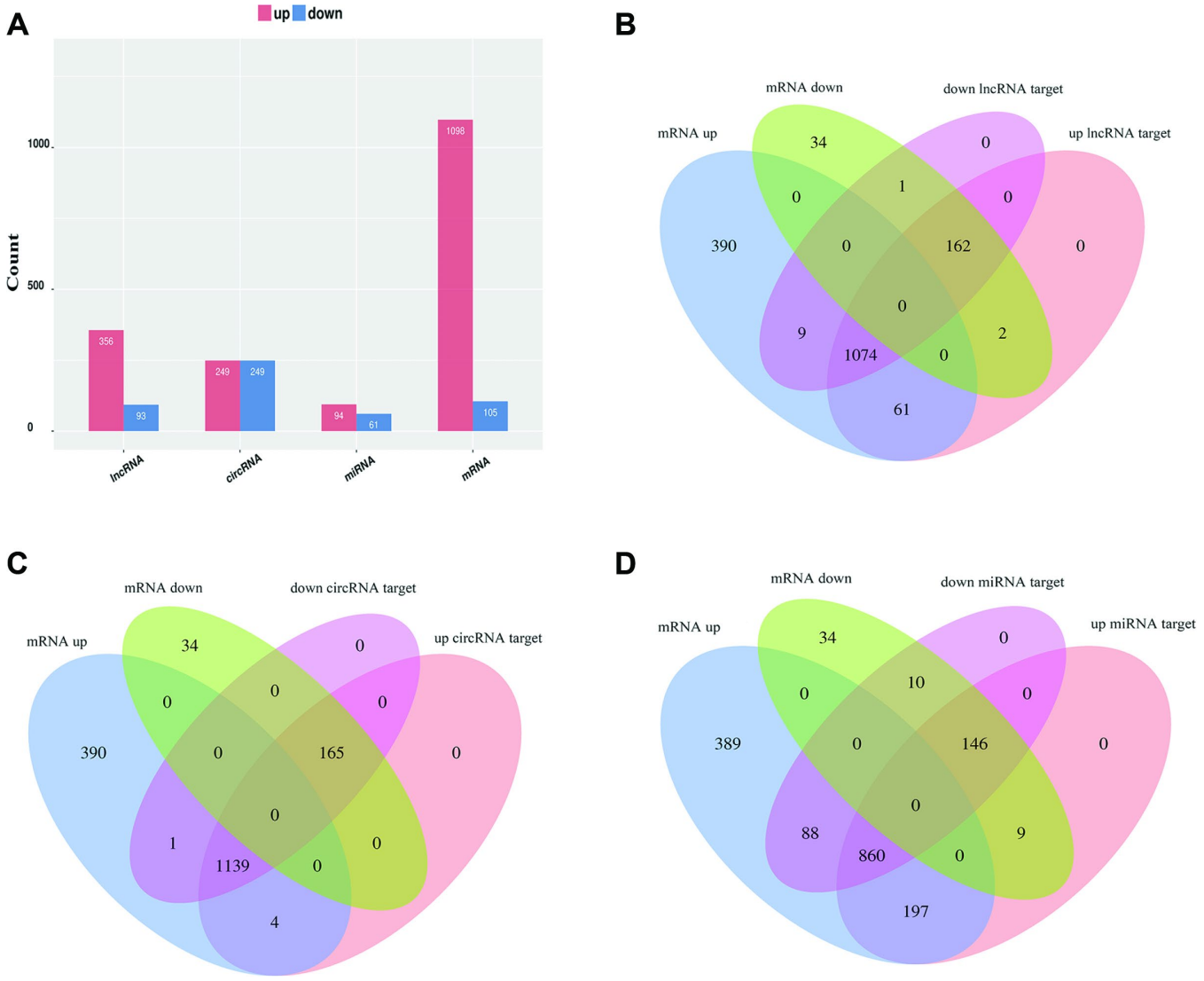

Figure 3. Overview of relative differential expression of ncRNAs. (**A**) Histogram showing the number of dysregulated ncRNAs and mRNAs. (**B**–**D**) Venn diagram showing the overlap between the target mRNAs of dysregulated ncRNAs and dysregulated mRNAs.

recent decades [19]. TSCI is a two-step process that can cause a permanent loss or reduction in bodily function below the level of the lesion site. The primary damage is the mechanical injury itself, and the secondary damage results from biochemical processes following the primary damage [3]. Physical trauma causes rupture of the blood-spinal cord barrier in the lesion epicenter, leading to hemorrhage, ischemia and inflammation, followed by local neuronal and glial cell death [5]. The nonneural damage in the lesion core ultimately resolves into a cavity surrounded by astrocytic and fibrotic scar borders [20]. Axonal regeneration is a complex procedure that includes structural synapse remodeling, axonal sprouting and regrowth across the lesion. A reduced intrinsic growth capacity, the absence of external growth stimulation and the presence of external inhibitory factors could lead to the failure of axons to regrow spontaneously across severe tissue lesions [21, 22]. The lesion compartments consist of different cell types, and cell biology influences axonal growth and regrowth in different ways [23]. Alleviating these differences is fundamental for achieving or improving axonal regeneration and designing rationally targeted interventions. Although several biomolecules are being used as diagnostic or prognostic biomarkers and therapeutic targets, they do not have sufficient accuracy or sensitivity to recognize pathogenesis, guide therapy or evaluate prognosis [5]. Since TSCI is a multifaceted pathological process, it is unlikely that any one molecule

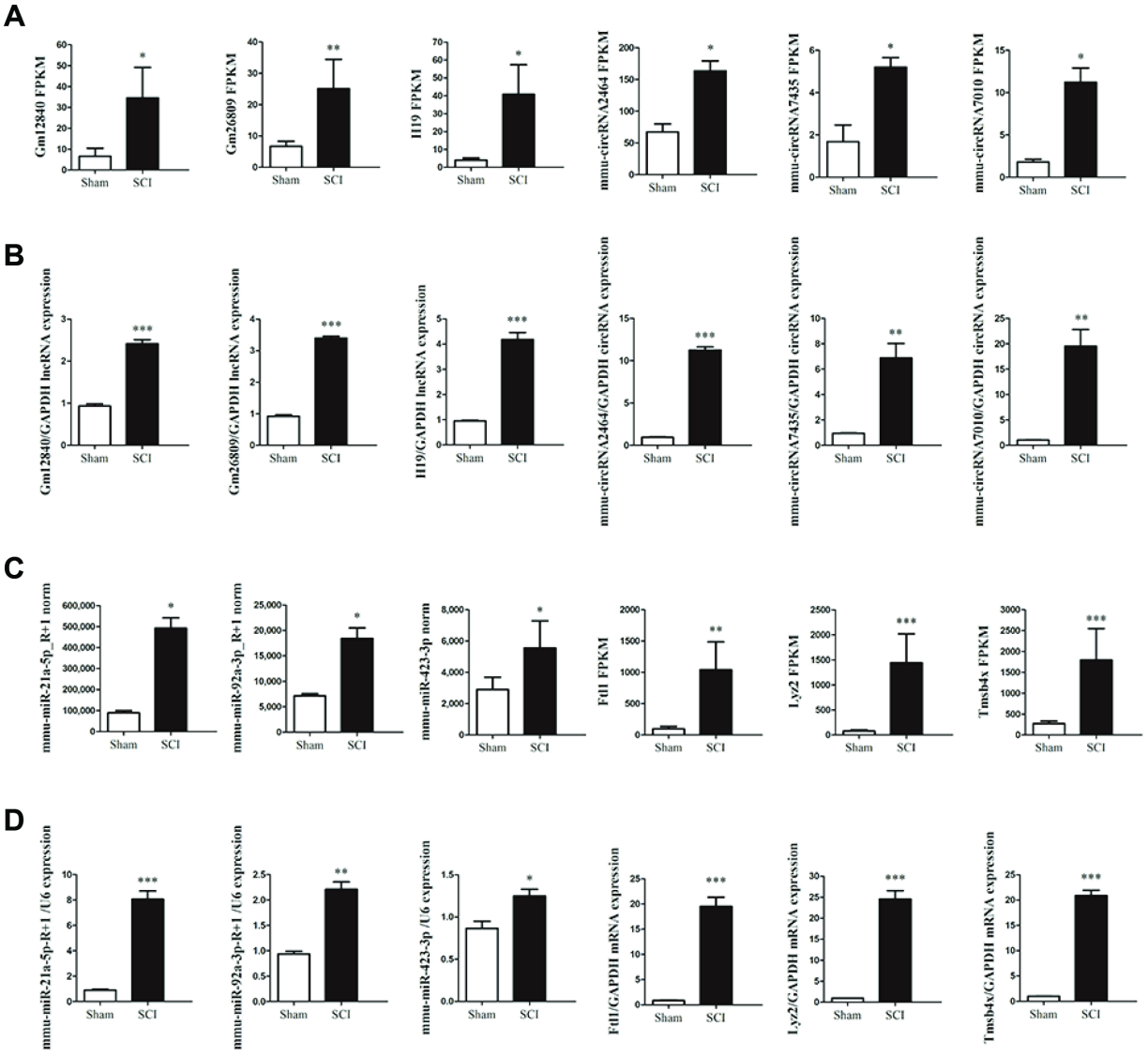

Figure 4. Validation of differential ncRNA and mRNA expression. (**A**, **C**) Sequencing results of the ncRNAs and mRNAs. (**B**, **D**) Expression of corresponding ncRNAs and mRNAs validated by qRT-PCR.

or pathway can affect the large number of obstacles that occur following trauma. Indeed, this may be the reason why many disparate treatments generate similar levels of recovery in TSCI animal models; as such, constructing the regulatory network involved with TSCI is clinically significant. In this study, we demonstrated that the expression of related ncRNAs and mRNAs significantly changes in the spinal cord tissue after traumatic injury, and we predicted the structure and potential functions of the regulatory network associated with these DE ncRNAs and mRNAs.

Recent studies have revealed the involvement of some specific miRNAs in many types of neuronal function in

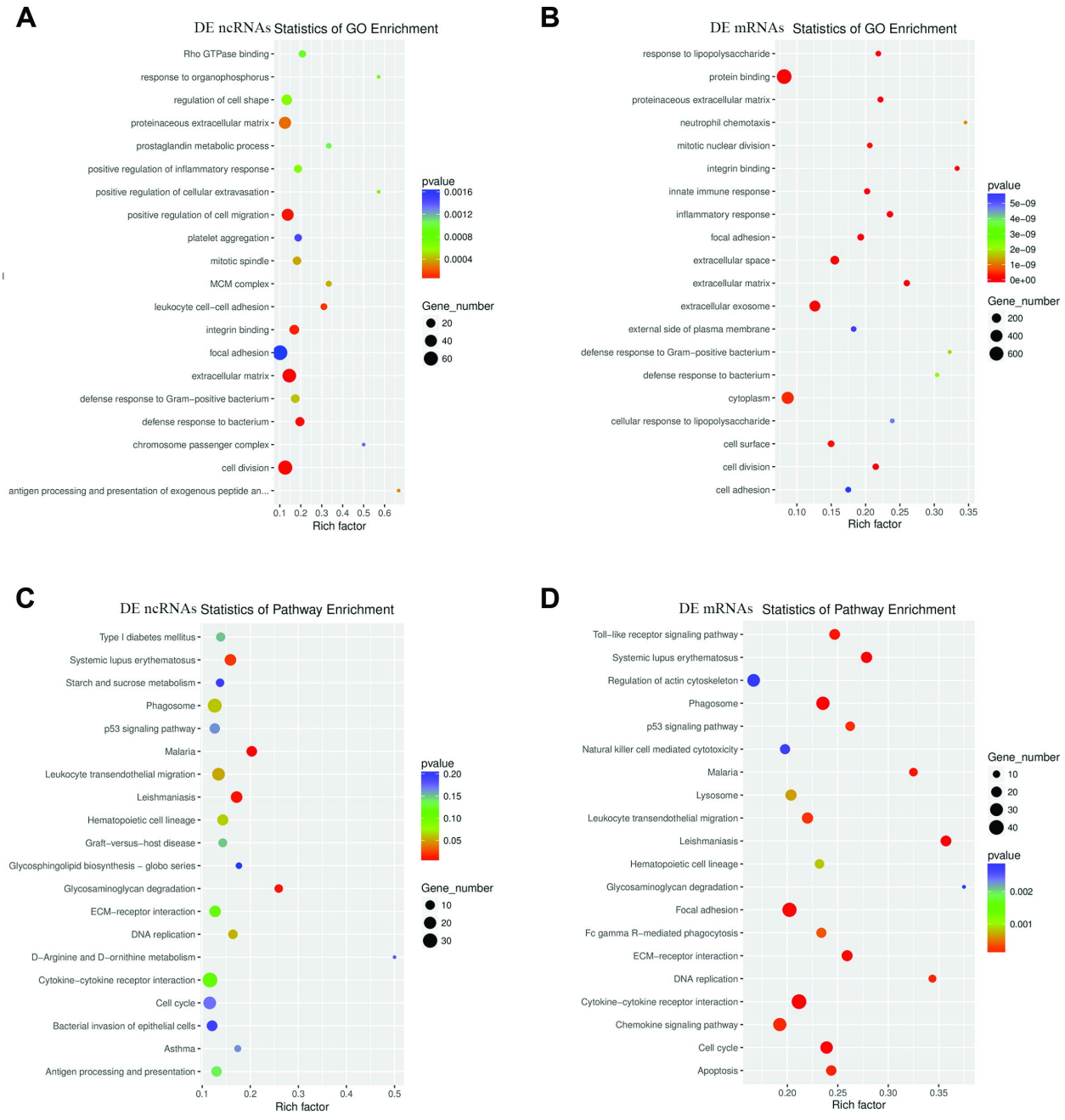

Figure 5. Enriched GO terms and KEGG pathways of host genes of DE ncRNAs in SCI mice. (**A**) Top 20 significantly enriched GO terms of DE ncRNAs are shown in the scatterplot. (**B**) Top 20 significantly enriched GO terms of DE mRNAs. (**C**) The top 20 significantly enriched KEGG pathways of DE ncRNAs are shown in the scatterplot. (**D**) The top 20 significantly enriched KEGG pathways of DE mRNAs are listed.

diseases, such as axon regrowth and neurodegeneration. MiRNAs are considered to be one of the major factors in the pathogenesis of CNS injury because of their intrinsic properties in regulating several biological functions and their potentially large impact in RNA disorders [24]. In this study, a marked dysregulating occurs in the expression of axon regrowth- or regeneration-associated mRNAs after injury, such as STAT3, p53, c-Jun, FOXO, KLFs and Sox, as well as their target DE miRNAs, miR-125b, miR-9, miR-222, miR-21, miR-135b and miR-145, respectively. In addition, miRNAs are critical regulators of the main molecular cascades regulating axonal growth, *i.e.*, miR-26a and miR-222 repress the PTEN pathway, miR-124 targets the GSK-3b pathway, miR-9 targets the MAP1B–Rac1 pathway, and miR-133 inhibits the rhoA–PI3K–AKT pathway. MiRNAs also participate in inflammation, apoptosis and myelination-related lesions in neurological damage disease, *i.e.*, let-7 inhibits IL-6 during inflammation, miR-29b increases proapoptotic gene expression, and miR-138 regulates myelination-related lesions.

Most strikingly, ceRNAs, which include lncRNAs, circRNAs and pseudogenic RNAs, cross-regulate each other by competing for shared miRNAs on miRNA response elements (MREs) [25]. CeRNA crosstalk is a type of posttranscriptional regulation that is mediated by miRNAs and links the functions of coding and noncoding RNAs. LncRNA can directly regulate the structure of DNA and the transcription and translation of RNA; notably, lncRNA can act as an miRNA sponge to competitively bind miRNA [14]. CircRNAs were later identified and are more enriched in neuronal tissues than other tissues because the long introns of neuronal genes promote circRNA formation [26]. The ceRNA regulation network plays a critical role in central neuropathy, i.e., the lncRNA

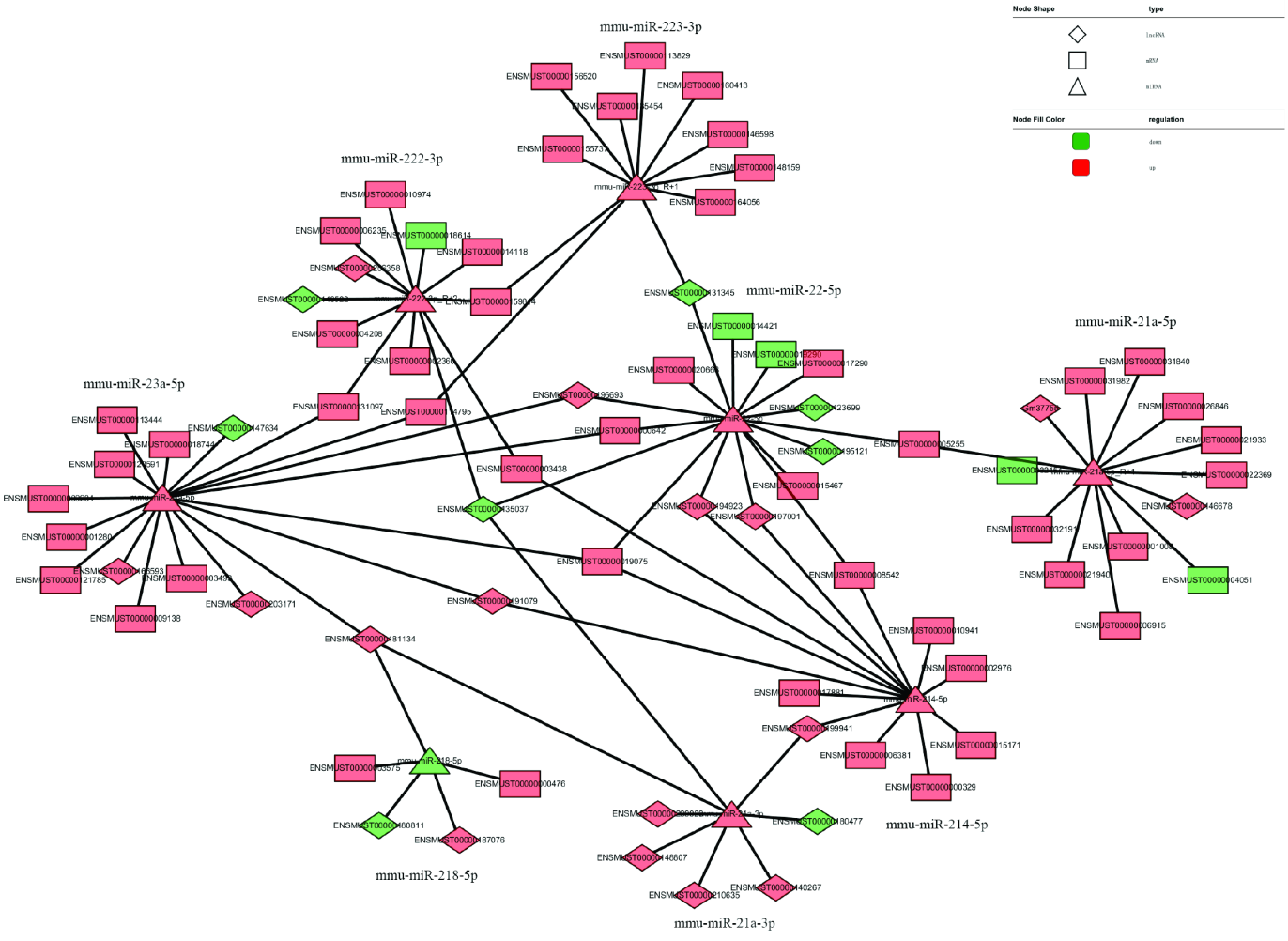

Figure 6. LncRNA–miRNA–mRNA regulatory interaction network analysis.

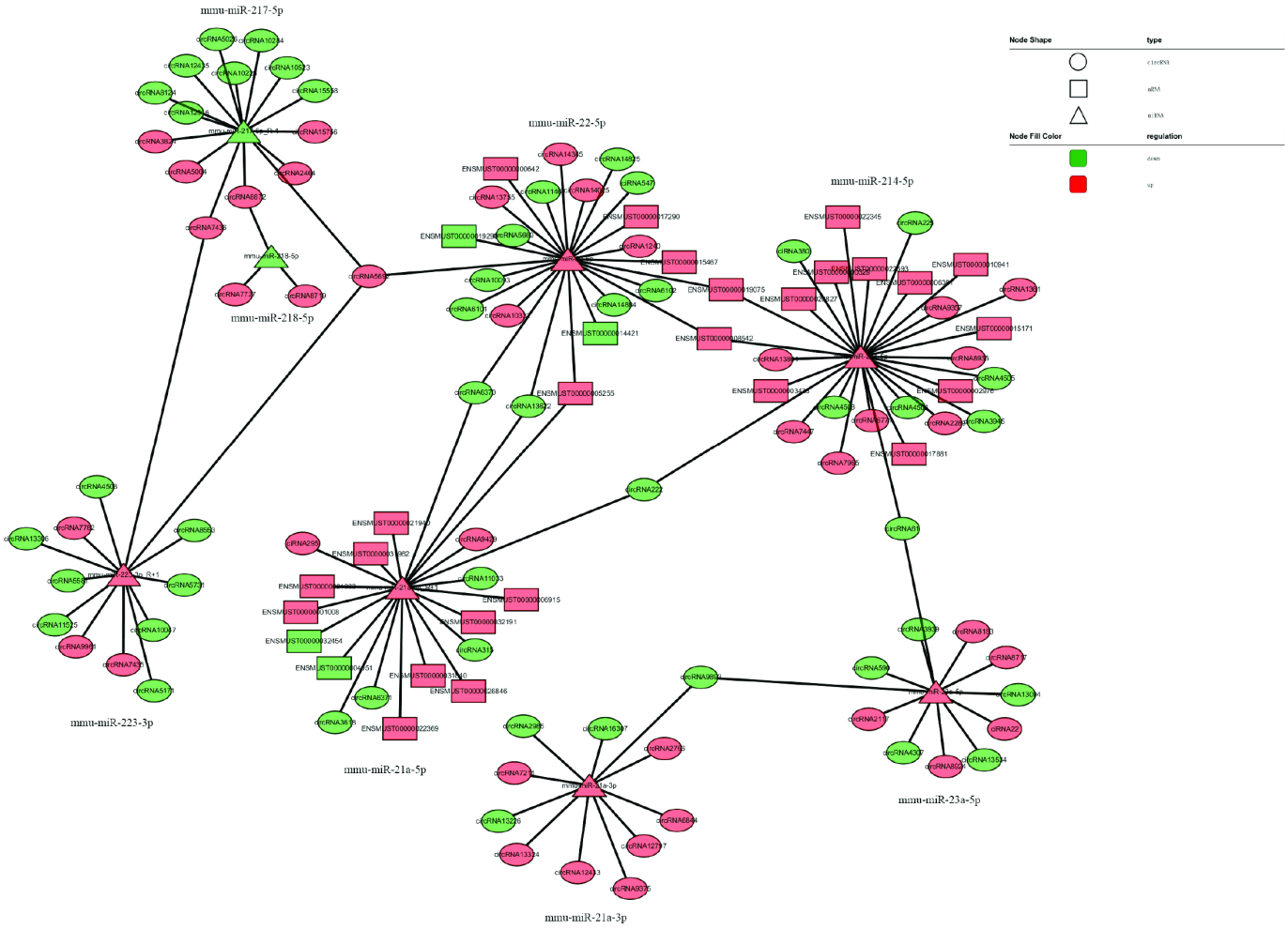

Figure 7. CircRNA–miRNA–mRNA regulatory interaction network analysis.

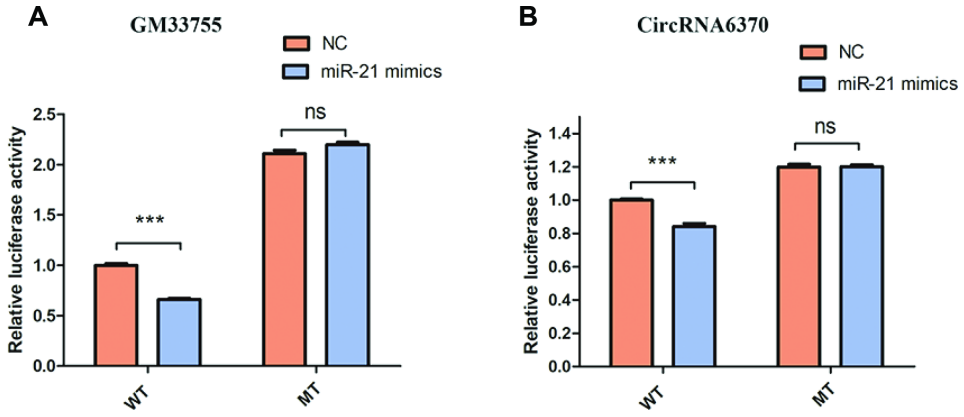

Figure 8. Confirmation of the relationships. (**A**) Relative luciferase expression of wild-type and mutant lncRNAGM33755 UTR-bearing luciferase vectors cotransfected with miR-135b expression vectors. (**B**) Relative luciferase expression of wild-type and mutant circRNA6370 UTR-bearing luciferase vectors cotransfected with miR-135b expression vectors. n=6, ***P<0.001.

SNHG5–KLF4–eNOS axis enhances the viability of astrocytes and microglia [27], the circRNA2837–miR-34a axis protects neurons against injury by inducing autophagy [28], and the circRNA ZNF609–miR-615–METRN axis reverses retinal neurodegeneration [29]. Recent research has even generated a complicated ceRNA network demonstrating that lncCyrano–miR-7 prevents the cytoplasmic destruction of circCdr1while repressing miR-671–circCdr1splicing in the brain [12]. In addition, to explore the roles of ncRNAs through this potential mechanism, we performed GO and KEGG pathway analysis to annotate predicted target mRNAs and predominant pathways of the differentially expressed ncRNAs. In this study, we found that the target mRNAs are involved in multiple biological processes, cellular signaling pathways, protein activities and gene splicing after SCI. Strikingly, focal adhesion was noted to be one of the most significantly enriched and meaningful terms of biological processes in both ncRNAs and mRNAs after GO analysis, and phagosome pathways was found to be one of the most significantly enriched and meaningful pathway of ncRNAs and mRNAs groups after KEGG pathway analysis.

In previous work, we demonstrated that miR-21 regulates astrogliosis through the PI3K–Akt–mTOR pathway and regulates fibrosis through the TGF-β–Smad pathway after TSCI [33, 30]. The reactive astrocytes and fibrotic scar tissue formed by perivascular cells stabilize the outer borders of the initial lesion epicenter and act as a chronic, physical, and chemical-entrapping barrier that prevents axonal regeneration [31, 32]. Our previous results suggest that miR-21 knockdown significantly suppressed scar formation and improved motor functional recovery after TSCI [30, 33]. In this article, a ceRNA regulation network with miR-21 as the center was constructed and provides initial evidence of the binding relationships between lncRNA GM33755, circRNA 6730 and miR-21. However, further specific studies are needed to determine whether lncRNA GM33755 and circRNA 6730 play roles in pathological processes after neurological injury.

Recently, our understanding of the extrinsic and intrinsic factors that block axonal regeneration or neuroplasticity has immensely improved with further illumination of the molecular events that occur following TSCI in mouse models. However, it is important to keep in mind that variations in axonal regeneration responses exist between mice and humans. In this article, we choose 3 days post-SCI as our time point, acute phase is the original point of pathological process. In acute phase, cell death and eventually axonal die back. Inflammation and axon regrowth at later time point, in sub-acute or chronic phases, then astrogliosis and fibrotic scar are done, axon struggle to regeneration. TSCI has an acute phase and a chronic phase, what should we do next is to compare different injuries severity in acute time points and chronic time points. Future efforts should be made to mimic endogenous ncRNA deregulation and determine the functions of ncRNA interactions in the context of posttranscriptional regulation as a whole. Findings arising from such studies will expand our understanding of the potential of ncRNAs, offer novel insight into the identification of new biomarkers and help guide strategies toward the development of potential therapies to enhance axonal regeneration and functional recovery during acute and chronic stages following TSCI. The spinal cord rarely repairs itself after an injury, but methods for promoting axonal regeneration are on the horizon.

MATERIALS AND METHODS

Mouse SCI model and experimental groups

All animal protocols were approved by the Research Ethics Committee of Shandong University (Jinan, China). All tissue samples of the SCI epicenter and parameters of Allen's weight-drop apparatus were obtained as described in our previous study [33]. Briefly, 64 adult male C57BL/6 mice were randomly divided into the SCI (n=8)×4 and sham (n=8)×4 groups. Mice in the SCI group underwent $T_{8–10}$ vertebral laminectomy to expose the spinal cord after anesthesia was induced with 3% pentobarbital. Then, moderate SCI was induced using a modified Allen's weight-drop apparatus, subsequently, the muscles and skin were sutured layer by layer. Mice in the sham group underwent the same laminectomy but without SCI. The movement ability of randomly selected mice (SCI group n=3, sham group n=3) was evaluated using the Basso motor score (BMS) for 3 days. Three independent and well-trained investigators scored the animals according to the standard guidelines. Then, the final score was recorded as the average of the investigators' scores. First batch of 16 C57BL/6 mice divided into the SCI group (n=4) and sham group (n=4), were humanely sacrificed on days 1 and 3 postsurgery, respectively, for the collection of $T_{8–10}$ spinal cord tissues. The spinal cord lesions were analyzed after tissue samples were fixed, washed, dehydrated, cleared, embedded, frozen and stained with H&E as previously described [33]. The remaining 48 mice, SCI (n=8)×3 and sham (n=8)×3, were humanely sacrificed on day 3 postsurgery for the collection of $T_{8–10}$ spinal cord samples, then used to extract total RNA for Sequencing and qRT-PCR validation.

RNA library construction and sequencing, transcript abundance estimation and differential expression analysis

Total RNA of spinal specimens was extracted using the TRIzol reagent (Invitrogen, Carlsbad, CA, USA). The

Table 5. Primers designed for qRT-PCR validation.

Gene	Primer
H19	**F** TTCACTTAGAAGAAGGTTCA **R** TTCCATTCTCCAGTTATTGA
Gm12840	**F** CCAAGGAGTTGACTGATTATCT **R** ACACAAGCAAGACCAATACA
Gm26809	**F** ATCTCTAAGCACACTCGTCCAC **R** ACTAATCGCCGCCGTCAG
circRNA7010	**F** CTGGAGACTGTGGAAAGC **R** TGTAAGGACACTGGGGC
circRNA2464	**F** CTGTCAAGTATGTGGAGTG **R** CAACAGCACCATCACC
circRNA7435	**F** ATGACATCCGCAGAAGG **R** AGGCAAATACCGCACTC
mmu-miR-21a-5p_R+1	**F** CGGGCGTAGCTTATCAGACTG **RT** GTCGTATCCAGTGCAGGGTCC GAGGTATTCGCACTGGATACGACGTCAAC
mmu-miR-423-3p	**F** TTAGCTCGGTCTGAGGCCC **RT** GTCGTATCCAGTGCAGGGTCC GAGGTATTCGCACTGGATAC GACACTGAG
mmu-miR-92a-3p	**F** CCGTATTGCACTTGTCCCG
	RT GTCGTATCCAGTGCAGGGTCC GAGGTATTCGCACTGGATAC GACACAGGC
Tmsb4x	**F** AGAACTACTGAGCAGGAAGG **R** GGACATCTTTGACCATCTTGAA
Lyz2	**F** ATGAAGACTCTCCTGACTCTG **R** ATAGTAGCCAGCCATTCCAT
Ftl1	**F** TGGAGAAGAACCTGAATCA **R** AGGAAGTCACAGAGATGAG
GAPDH	**F** GGTGAAGGTCGGTGTGAACG **R** CTCGCTCCTGGAAGATGGTG
U6	**F** CTCGCTTCGGCAGCACATATACT **R** ACGCTTCACGAATTTGCGTGTC

procedure mainly included homogenization, phase separation, RNA precipitation, washing, solubilization, and monitoring of RNA degradation. The RNA concentration and quality were measured by UV absorbance at 260/280 nm; then, a LabChip Kit (Agilent, CA, USA) was used to analyze the RNA integrity.

Small RNA single-end sequencing was performed on an Illumina HiSeq 2500 LC-BIO system (Hangzhou, China). CircRNA and lncRNA paired-end sequencing were performed on an Illumina HiSeq 4000 LC-BIO system (Hangzhou, China). The fragments per kilobase of exon per million fragments mapped (FPKM) was used to measure the relative abundance of the transcripts after aligned read files were processed by in-house scripts. The expression levels of lncRNAs and mRNAs were determined by StringTie (http://ccb.jhu.edu/software/stringtie). CIRCexplorer was used to measure the expression of circRNAs [34], unique circRNAs were generated from assemblies.

qRT-PCR validation

As previously described [35], total RNA was reverse-transcribed into cDNA; then qRT-PCR was performed using an Applied Biosystems (Wilmington, DE, USA) 7500 RT-PCR system. GAPDH was used as an internal control to normalize relative circRNA, lncRNA and mRNA expression levels. MiRNA expression levels were normalized using U6. The $2^{-\Delta\Delta CT}$ method was used for comparative quantitation. Three independent experiments were performed. The specific primers for each gene are listed in Table 5.

GO annotations and KEGG pathway analysis

GO annotations and KEGG pathway analysis were performed to investigate the potential roles of all DE ncRNAs. GO analysis includes three domains, cellular components, biological processes, and molecular functions, and provides a controlled vocabulary to describe DE mRNAs ($P<0.05$) in GO categories (http://www.geneontology.org) [36]. In addition, the KEGG database (http://www.genome.ad.jp/kegg/) was used to detect the potential functions of the target genes in the identified pathways [37], with significance indicated by P-values <0.05.

Analysis of ncRNA regulatory network

An ncRNA regulatory network was constructed to examine the interactions and functional links among dysregulated mRNAs and ncRNAs in the pathological process of SCI. The target mRNAs of miRNA were predicted by software programs as previously described [35]. We selected the dysregulated target RNAs correlating to DE ncRNAs. Cytoscape software (San Diego, CA, USA) was used to construct interaction networks for lncRNA–miRNA–mRNA and circRNA–miRNA–mRNA.

Luciferase assay

293T cells were cultured in 94-well plates and cotransfected with luciferase reporter constructs containing lncRNA GM33755 or circRNA 6370 (LC) and a Renilla luciferase construct (Invitrogen), miRNA-21 mimic or scrambled negative control (LC) were transfected using Lipofectamine 2000 (Invitrogen) for 6 h. After 48 h of culture at 37°C, the culture supernatant was mixed with LAR II and measured using an illuminometer. Then, a luciferase activity assay was performed using a dual luciferase reporter system (E1910, Promega, Madison, WI, USA). In addition, Stop&Glo Reagent used as an internal control. The results shown represent the means of three experiments and are presented as the mean ± standard deviation (SD).

Statistical analysis

SPSS 20.0 (IBM, Chicago, IL, USA) and GraphPad Prism software (La Jolla, CA, USA) were used to perform the statistical analysis. Data are presented as the mean ± SD. ANOVA and Student's t-test were used for comparisons ($P<0.05$). The Chi-squared 2X2 test, Chi-squared nXn test and Fisher's exact test were used to assess the differential expression of miRNA ($P<0.05$), differential lncRNAs expression was examined using the R package Ballgown ($P<0.05$) and CircRNA expression in the different samples and groups was calculated using scripts developed in-house ($P<0.05$).

Ethical disclosure

The authors state that the study was approved by the Ethics Committee of Jinan Central Hospital Affiliated to Shandong University.

AUTHOR CONTRIBUTIONS

W.W. performed the experiments. Y.S. and T.S. were responsible for construction of the animal model, collection of the results and analysis of the ncRNA regulatory network. H.L. and W.X. were responsible for the PCR and luciferase assays. J.C., X.P. and L.S. participated in the data analysis. B.N. conceived of the study and participated in its design and coordination. All authors have read and approved the final submitted manuscript.

CONFLICTS OF INTEREST

Grant support was provided by the National Natural Science Fund of China (Nos. 81401014, 81771346), the Chinese Postdoctoral Science Foundation (No. 2014M561935), the Chinese Postdoctoral Science Foundation (No. 2015T80725), and Technology Research and Development Program of Jinan City (No. 201704133).

REFERENCES

1. Fouad K, Krajacic A, Tetzlaff W. Spinal cord injury and plasticity: opportunities and challenges. Brain Res Bull. 2011; 84:337–42. https://doi.org/10.1016/j.brainresbull.2010.04.017

2. Holmes D. Spinal-cord injury: spurring regrowth. Nature. 2017; 552:S49. https://doi.org/10.1038/d41586-017-07550-9

3. Cristante AF, Barros Filho TE, Marcon RM, Letaif OB, Rocha ID. Therapeutic approaches for spinal cord injury. Clinics (São Paulo). 2012; 67:1219–24. https://doi.org/10.6061/clinics/2012(10)16

4. van Middendorp JJ, Barbagallo G, Schuetz M, Hosman AJ. Design and rationale of a Prospective, Observational European Multicenter study on the efficacy of acute surgical decompression after traumatic Spinal Cord Injury: the SCI-POEM study. Spinal Cord. 2012; 50:686–94. https://doi.org/10.1038/sc.2012.34

5. Tran AP, Warren PM, Silver J. The Biology of Regeneration Failure and Success After Spinal Cord Injury. Physiol Rev. 2018; 98:881–917. https://doi.org/10.1152/physrev.00017.2017

6. Geng Y, Jiang J, Wu C. Function and clinical significance of circRNAs in solid tumors. J Hematol Oncol. 2018; 11:98. https://doi.org/10.1186/s13045-018-0643-z

7. Djebali S, Davis CA, Merkel A, Dobin A, Lassmann T, Mortazavi A, Tanzer A, Lagarde J, Lin W, Schlesinger F, Xue C, Marinov GK, Khatun J, et al. Landscape of transcription in human cells. Nature. 2012; 489:101–08. https://doi.org/10.1038/nature11233

8. Qu S, Yang X, Li X, Wang J, Gao Y, Shang R, Sun W, Dou K, Li H. Circular RNA: A new star of noncoding RNAs. Cancer Lett. 2015; 365:141–48. https://doi.org/10.1016/j.canlet.2015.06.003

9. Berindan-Neagoe I, Monroig PC, Pasculli B, Calin GA. MicroRNAome genome: a treasure for cancer diagnosis and therapy. CA Cancer J Clin. 2014; 64:311–36. https://doi.org/10.3322/caac.21244

10. Ameres SL, Zamore PD. Diversifying microRNA sequence and function. Nat Rev Mol Cell Biol. 2013; 14:475–88. https://doi.org/10.1038/nrm3611

11. Stoicea N, Du A, Lakis DC, Tipton C, Arias-Morales CE, Bergese SD. The MiRNA Journey from Theory to Practice as a CNS Biomarker. Front Genet. 2016; 7:11. https://doi.org/10.3389/fgene.2016.00011

12. Kleaveland B, Shi CY, Stefano J, Bartel DP. A Network of Noncoding Regulatory RNAs Acts in the Mammalian Brain. Cell. 2018; 174:350–362.e17. https://doi.org/10.1016/j.cell.2018.05.022

13. Calin GA, Liu CG, Ferracin M, Hyslop T, Spizzo R, Sevignani C, Fabbri M, Cimmino A, Lee EJ, Wojcik SE, Shimizu M, Tili E, Rossi S, et al. Ultraconserved regions encoding ncRNAs are altered in human leukemias and carcinomas. Cancer Cell. 2007; 12:215–29. https://doi.org/10.1016/j.ccr.2007.07.027

14. Kopp F, Mendell JT. Functional Classification and Experimental Dissection of Long Noncoding RNAs. Cell. 2018; 172:393–407. https://doi.org/10.1016/j.cell.2018.01.011

15. Zhang Z, Yang T, Xiao J. Circular RNAs: Promising Biomarkers for Human Diseases. EBioMedicine. 2018; 34:267–74. https://doi.org/10.1016/j.ebiom.2018.07.036

16. Garfin SR, Yuan HA, Reiley MA. New technologies in spine: kyphoplasty and vertebroplasty for the treatment of painful osteoporotic compression fractures. Spine. 2001; 26:1511–15. https://doi.org/10.1097/00007632-200107150-00002

17. Jensen ME, Evans AJ, Mathis JM, Kallmes DF, Cloft HJ, Dion JE. Percutaneous polymethylmethacrylate vertebroplasty in the treatment of osteoporotic vertebral body compression fractures: technical aspects. AJNR Am J Neuroradiol. 1997; 18:1897–904.

18. Alexandru D, So W. Evaluation and management of vertebral compression fractures. Perm J. 2012; 16:46–51. https://doi.org/10.7812/TPP/12-037

19. Schwab JM, Maas AI, Hsieh JT, Curt A. Raising awareness for spinal cord injury research. Lancet Neurol. 2018; 17:581–82. https://doi.org/10.1016/S1474-4422(18)30206-0

20. Dias DO, Kim H, Holl D, Werne Solnestam B, Lundeberg J, Carlen M, Goritz C, Frisen J. Reducing Pericyte-Derived Scarring Promotes Recovery after Spinal Cord Injury. Cell. 2018; 173: 153–165.e22. https://doi.org/10.1016/j.cell.2018.02.004

21. Anderson MA, Burda JE, Ren Y, Ao Y, O'Shea TM, Kawaguchi R, Coppola G, Khakh BS, Deming TJ, Sofroniew MV. Astrocyte scar formation aids central nervous system axon regeneration. Nature. 2016; 532:195–200. https://doi.org/10.1038/nature17623

22. Stroman PW, Khan HS, Bosma RL, Cotoi AI, Leung R, Cadotte DW, Fehlings MG. Changes in Pain Processing in the Spinal Cord and Brainstem after Spinal Cord Injury Characterized by Functional Magnetic Resonance Imaging. J Neurotrauma. 2016; 33:1450–60. https://doi.org/10.1089/neu.2015.4257

23. Sofroniew MV. Dissecting spinal cord regeneration. Nature. 2018; 557:343–50. https://doi.org/10.1038/s41586-018-0068-4

24. Ghibaudi M, Boido M, Vercelli A. Functional integration of complex miRNA networks in central and peripheral lesion and axonal regeneration. Prog Neurobiol. 2017; 158:69–93. https://doi.org/10.1016/j.pneurobio.2017.07.005

25. Qi X, Zhang DH, Wu N, Xiao JH, Wang X, Ma W. ceRNA in cancer: possible functions and clinical implications. J Med Genet. 2015; 52:710–18. https://doi.org/10.1136/jmedgenet-2015-103334

26. Chen W, Schuman E. Circular RNAs in Brain and Other Tissues: A Functional Enigma. Trends Neurosci. 2016; 39:597–604. https://doi.org/10.1016/j.tins.2016.06.006

27. Jiang ZS, Zhang JR. LncRNA SNHG5 enhances astrocytes and microglia viability via upregulating KLF4 in spinal cord injury. Int J Biol Macromol. 2018; 120:66–72. https://doi.org/10.1016/j.ijbiomac.2018.08.002

28. Zhou ZB, Niu YL, Huang GX, Lu JJ, Chen A, Zhu L. Silencing of circRNA.2837 Plays a Protective Role in Sciatic Nerve Injury by Sponging the miR-34 Family via Regulating Neuronal Autophagy. Mol Ther Nucleic Acids. 2018; 12:718–29. https://doi.org/10.1016/j.omtn.2018.07.011

29. Wang JJ, Liu C, Shan K, Liu BH, Li XM, Zhang SJ, Zhou RM, Dong R, Yan B, Sun XH. Circular RNA-ZNF609 regulates retinal neurodegeneration by acting as miR-615 sponge. Theranostics. 2018; 8:3408–15. https://doi.org/10.7150/thno.25156

30. Liu R, Wang W, Wang S, Xie W, Li H, Ning B. microRNA-21 regulates astrocytic reaction post-acute phase of spinal cord injury through modulating TGF-β signaling. Aging (Albany NY). 2018; 10:1474–88. https://doi.org/10.18632/aging.101484

31. Hara M, Kobayakawa K, Ohkawa Y, Kumamaru H, Yokota K, Saito T, Kijima K, Yoshizaki S, Harimaya K, Nakashima Y, Okada S. Interaction of reactive astrocytes with type I collagen induces astrocytic scar formation through the integrin-N-cadherin pathway after spinal cord injury. Nat Med. 2017; 23:818–28. https://doi.org/10.1038/nm.4354

32. Catenaccio A, Llavero Hurtado M, Diaz P, Lamont DJ, Wishart TM, Court FA. Molecular analysis of axonal-intrinsic and glial-associated co-regulation of axon degeneration. Cell Death Dis. 2017; 8:e3166. https://doi.org/10.1038/cddis.2017.489

33. Wang W, Liu R, Su Y, Li H, Xie W, Ning B. MicroRNA-21-5p mediates TGF-β-regulated fibrogenic activation of spinal fibroblasts and the formation of fibrotic scars after spinal cord injury. Int J Biol Sci. 2018; 14:178–88. https://doi.org/10.7150/ijbs.24074

34. Zhang XO, Wang HB, Zhang Y, Lu X, Chen LL, Yang L. Complementary sequence-mediated exon circularization. Cell. 2014; 159:134–47. https://doi.org/10.1016/j.cell.2014.09.001

35. Wang W, Tang S, Li H, Liu R, Su Y, Shen L, Sun M, Ning B. MicroRNA-21a-5p promotes fibrosis in spinal fibroblasts after mechanical trauma. Exp Cell Res. 2018; 370:24–30. https://doi.org/10.1016/j.yexcr.2018.06.002

36. Gene Ontology C, and Gene Ontology Consortium. Gene Ontology Consortium: going forward. Nucleic Acids Res. 2015; 43:D1049–56. https://doi.org/10.1093/nar/gku1179

37. Kanehisa M, Araki M, Goto S, Hattori M, Hirakawa M, Itoh M, Katayama T, Kawashima S, Okuda S, Tokimatsu T, Yamanishi Y. KEGG for linking genomes to life and the environment. Nucleic Acids Res. 2008; 36:D480–84. https://doi.org/10.1093/nar/gkm882